TIME-VARYING WAVEFORM SELECTION AND CONFIGURATION FOR AGILE SENSORS IN TRACKING APPLICATIONS

Sandeep P. Sira, Antonia Papandreou-Suppappola and Darryl Morrell

Department of Electrical Engineering, Arizona State University

ABSTRACT

In this paper, we present an algorithm for dynamic waveform selection and configuration for agile sensors in a target tracking application. The method selects and configures generalized frequency-modulated (FM) waveforms with time-varying signatures to minimize predicted mean squared tracking error. We derive the Cramer-Rao lower bound (CRLB) for these signals and use the CRLB in conjunction with the unscented transform to compute the predicted mean square error. The method is computationally feasible and applicable to nonlinear scenarios as demonstrated in our simulations.

1. INTRODUCTION

Agile sensors use waveforms that can change from pulse to pulse to match the target or the environment in order to improve system performance. In tracking applications, for example, the transmitted waveform can be designed and its parameters optimally selected to reduce resource costs and maximize performance criteria. Thus, it is important to select the appropriate pulses on the fly and to design algorithms for optimal waveform scheduling at the sensor front-end to best perform a specified task.

Dynamic waveform selection can significantly improve system performance in several applications. For example, optimal waveform selection for target detection over a finite horizon using stochastic dynamic programming was addressed in [1]. In [2, 3], the authors considered the problem of optimal waveform selection to track a target using a sensor that chooses waveform parameters to minimize the error variance of the estimate of the target state vector. The target motion was one-dimensional, which allowed the use of a Kalman filter tracker and resulted in closed form relationships between the waveform parameters and the cost functional to be minimized. As a consequence, their solution cannot be extended to more complex target motions. In [4], this work was extended to tracking a target using a probabilistic data association filter in the presence of clutter.

In this paper, we consider tracking a target moving in two-dimensions (2-D) using a class of generalized FM (GFM) chirp signals. These signals are time-varying (TV) as their frequency content changes nonlinearly with time. The varying waveform signatures have different supports in the time-frequency plane and thus bandwidths that depend on distinct waveform parameters. Also, GFM chirps such as linear and hyperbolic chirps have been shown to provide more accurate estimates of range and Doppler in sonar applications than signals with constant signatures [5].

We propose a configuration algorithm for waveform design and scheduling that selects a waveform and its parameters to minimize the predicted mean square tracking error. We use the CRLB, which we derive for GFM chirps, in conjunction with the unscented transform (UT) [6] to compute the predicted mean square error. Our configuration algorithm can be applied to any signal for which the CRLB can be computed and is feasible for real-time implementation.

2. PROBLEM FORMULATION

2.1. GFM waveform class

The target is tracked by two sensors, A and B, and each sensor transmits a waveform with various parameters. We consider a class of GFM waveforms, with complex Gaussian envelopes, that are defined as

$$s(t) = \left(\frac{1}{\pi\lambda^2}\right)^{\frac{1}{4}} \mathrm{e}^{-\frac{(t/t_r)^2}{2\lambda^2}} \mathrm{e}^{j2\pi b\xi(t/t_r)}. \qquad (1)$$

Here, λ parameterizes the duration of the Gaussian envelope, b is the FM rate, $\xi(t)$ is a real-valued, differentiable phase function and $t_r = 1$ is a reference time. Some examples of GFM waveforms include the linear FM (LFM), hyperbolic FM (HFM) and exponential FM (EFM) waveforms. They are defined in (1) with phase function, $\xi(t)$, and bandwidth, B, for an effective pulse length T_s, as summarized in Table 1. These waveforms have distinct TV signatures in the time-frequency plane that are obtained by the derivative of $\xi(t)$. For sensor i, i = A, B, $\boldsymbol{\theta}_k^i = [\lambda_k^i, b_k^i]^T$ represents the GFM waveform parameter vector at time k. We also consider the amplitude-only modulated Gaussian waveform defined as in (1) with $\xi(t) = t_r$ and $\boldsymbol{\theta}_k^i = \lambda_k^i$.

This work was supported by the DARPA ISP program through a contract with Raytheon Missile Systems.

Waveform	Phase Function, $\xi(t)$	Bandwidth, B
LFM	t^2	bT_s
HFM	$\ln(T+\|t\|), T>0$	b/T
EFM	$\mathrm{e}^{\|t\|}$	$b\mathrm{e}^{T_s/2}$

Table 1. Phase function and bandwidth of GFM waveforms.

2.2. State-Space model

The target dynamics are modeled using a linear, constant velocity model. Let $\mathbf{X}_k = [x_k \ y_k \ \dot{x}_k \ \dot{y}_k]^T$ represent the state of a target at time k, where x_k and y_k are the x and y position coordinates respectively, and $\dot{x}_k$ and $\dot{y}_k$ are the respective velocities. The target dynamics model and observation $\mathbf{Z}_k$ are

$$\mathbf{X}_k = F\,\mathbf{X}_{k-1} + \mathbf{W}_k, \quad \mathbf{Z}_k = h(\mathbf{X}_k) + \mathbf{V}_k\ , \qquad (2)$$

where target acceleration is modeled by $\mathbf{W}_k$, a zero-mean, Gaussian noise process with covariance matrix Q. F and Q are defined in [7]. Sensor i measures the time delay τ^i and Doppler shift ν^i of the received signal. The range and range-rate of the target are given by $r^i = c\tau^i/2$ and $\dot{r}^i = c\nu^i/(2\omega_c)$, where c is the velocity of propagation of the waveform and ω_c is the carrier frequency. The nonlinear relation between $\mathbf{X}_k$ and $\mathbf{Z}_k$ is given by $h(\mathbf{X}_k) = [r_k^A \ \dot{r}_k^A \ r_k^B \ \dot{r}_k^B]^T$ where

$$\begin{aligned} r_k^i &= \sqrt{(x_k - x^i)^2 \ + \ (y_k - y^i)^2} \\ \dot{r}_k^i &= (\dot{x}_k(x_k - x^i) + \dot{y}_k(y_k - y^i))/r^i. \end{aligned}$$

The measurement errors are modeled by $\mathbf{V}_k$, a zero-mean, Gaussian noise process with covariance matrix $N(\boldsymbol{\theta}_k)$. Here, $\boldsymbol{\theta}_k = [\boldsymbol{\theta}_k^{A^T} \boldsymbol{\theta}_k^{B^T}]^T$ is a combined waveform parameter vector for both sensors at time k. The measurement error thus depends explicitly upon the transmitted waveform. Due to the nonlinearity in the observation model, we use a particle filter to recursively estimate the target state [8].

2.3. Cost function minimization

Given the sequence of observations up to time $k-1$, we want to find the waveform and its parameters that minimize the predicted mean square tracking error at time k:

$$J(\boldsymbol{\theta}_k) = E_{\mathbf{X}_k,\mathbf{Z}_k|\mathbf{Z}_{1:k-1}}\left\{(\mathbf{X}_k - \hat{\mathbf{X}}_k)^T(\mathbf{X}_k - \hat{\mathbf{X}}_k)\right\}, \qquad (3)$$

where $E\{\cdot\}$ is the expectation over $\mathbf{X}_k$ and $\mathbf{Z}_k$, and $\hat{\mathbf{X}}_k$ is the estimate of $\mathbf{X}_k$ given the sequence of observations from 1 to k that is obtained by the particle filter. The sensors are configured at each time k to minimize $J(\boldsymbol{\theta}_k)$ in (3) by appropriately selecting a waveform and its parameter $\boldsymbol{\theta}_k$.

3. CRLB FOR GFM PULSES

In this section, we derive the relationship between the measurement errors and the waveform. From the narrowband ambiguity function (AF), we first derive the CRLB on the estimation errors for range and range-rate when the GFM waveforms are used. The CRLB is a suitable characterization of the optimal receiver under conditions of high signal-to-noise ratio (SNR) as the CRLB is shown to be related to the measurement error covariance $N(\boldsymbol{\theta}_k)$.

The ambiguity function of a signal $s(t)$ is $AF_s(\tau,\nu) = \int_{-\infty}^{\infty} s\left(t+\frac{\tau}{2}\right) s^*\left(t-\frac{\tau}{2}\right) e^{-j2\pi\nu t}dt$, where τ and ν can correspond to the errors in the estimates of the delay and Doppler shift of the pulse when reflected off the target. The negative of the second derivatives of the AF, evaluated at $\tau = 0, \nu = 0$, yield the elements of the Fisher information matrix (FIM) [9]. Denoting the SNR as η, the FIM is

$$I = \eta \begin{bmatrix} \frac{1}{2\lambda^2} + g(\xi) & 2\pi f(\xi) \\ 2\pi f(\xi) & (2\pi)^2\frac{\lambda^2}{2} \end{bmatrix}.$$

We computed its elements for the GFM pulse in (1) as

$$\begin{aligned} -\left.\frac{\partial^2 AF_s(\tau,\nu)}{\partial\tau^2}\right|_{\substack{\tau=0\\\nu=0}} &= \frac{1}{2\lambda^2} + g(\xi) \\ -\left.\frac{\partial^2 AF_s(\tau,\nu)}{\partial\tau\partial\nu}\right|_{\substack{\tau=0\\\nu=0}} &= 2\pi f(\xi) \\ -\left.\frac{\partial^2 AF_s(\tau,\nu)}{\partial\nu^2}\right|_{\substack{\tau=0\\\nu=0}} &= (2\pi)^2\frac{\lambda^2}{2}, \quad \text{where} \\ g(\xi) &= (2\pi b)^2\int_{-\infty}^{\infty}\frac{1}{\lambda\sqrt{\pi}}\mathrm{e}^{-\frac{t^2}{\lambda^2}}[\xi'(t)]^2dt\,, \qquad (4) \\ f(\xi) &= 2\pi b\int_{-\infty}^{\infty}\frac{t}{\lambda\sqrt{\pi}}\mathrm{e}^{-\frac{t^2}{\lambda^2}}\xi'(t)dt\,, \qquad (5) \end{aligned}$$

and $\xi'(t) = d\xi(t)/dt$. The CRLB on the variance of the error in the estimate of $[\tau,\nu]^T$ is given by I^{-1}. In a matched-filter receiver, the maximum likelihood estimates are jointly asymptotically Gaussian with covariance matrix I^{-1} [9]. We restrict our attention to cases where the SNR is high and there is no clutter. Hence, the side lobes of the AF may be neglected, and I^{-1} becomes a suitable characterization of the optimal receiver.

Since $r = c\tau/2$ and $\dot{r} = c\nu/(2\omega_c)$, the CRLB on the error variance of the estimate of $[r,\dot{r}]^T$ is given by $\Gamma I^{-1}\Gamma^T$ where $\Gamma = \mathrm{diag}(c/2, c/(2\omega_c))$. I^{-1} depends explicitly on the waveform parameters due to (4) and (5), and the measurement error covariance at the ith sensor is $N(\boldsymbol{\theta}_k^i) = \Gamma(I_k^i)^{-1}\Gamma^T$. We assume that the noise at each sensor is independent and hence $N(\boldsymbol{\theta}_k) = \mathrm{diag}(N(\boldsymbol{\theta}_k^A), N(\boldsymbol{\theta}_k^B))$.

4. WAVEFORM SELECTION USING THE UT

We use the unscented particle filter [8] to compute the probability density of the target state conditioned on the

observations. The waveform selection is accomplished by a grid search over all possible waveforms and their parameters. At each point of the grid, the expected cost in (3) is approximated using the UT [6] as follows.

Let $P_{xx}(k-1|k-1)$ represent the error covariance of the estimate of the state given the observations through $k-1$. We first predict the error covariance at time k using the dynamics model in (2):

$$P_{xx}(k|k-1) = FP_{xx}(k-1|k-1)F^T + Q.$$

To implement the UT, we select $n+1$ sigma points $\boldsymbol{\chi}_j$, $j = 0, 1, \ldots, n$ and corresponding weights. A transformed set of sigma points $\boldsymbol{\mathcal{Z}}_j = h(\boldsymbol{\chi}_j)$ is computed. Then, we calculate P_{zz}, the covariance of $\boldsymbol{\mathcal{Z}}_j$, and P_{xz}, the cross covariance between $\boldsymbol{\chi}_j$ and $\boldsymbol{\mathcal{Z}}_j$, using the sigma points and the weights [6].

Let $\boldsymbol{\theta}(l)$ represent the lth waveform parameter vector, $l = 0, \ldots, L-1$, with the corresponding noise covariance $N(\boldsymbol{\theta}(l))$ calculated as in Section 3. The estimate error covariance for $\boldsymbol{\theta}(l)$ is

$$P^l_{xx}(k|k) = P_{xx}(k|k-1) - P_{xz}\left[P_{zz} + N(\boldsymbol{\theta}(l))\right]^{-1} P^T_{xz},$$

and the approximate expected cost is given by $\hat{J}(\boldsymbol{\theta}(l)) = \text{Trace}\{P^{(l)}_{xx}(k|k)\}$. For each parameter vector $\boldsymbol{\theta}(l)$, $l = 0, \ldots, L-1$, $\hat{J}(\boldsymbol{\theta}(l))$ is calculated and the configuration that results in the least cost is selected as $\boldsymbol{\theta}_k$.

To implement the grid search, we form L combinations of waveform parameter vectors by varying λ and b for each waveform. The grid point spacing for λ and b is

$$\lambda(r) = \lambda_{min} + \frac{r(\lambda_{max} - \lambda_{min})}{R-1}, r = 0, \ldots, R-1 \quad (6)$$

$$b(m) = -b_{max} + \frac{m2b_{max}}{M-1},\ m = 0, \ldots, M-1. \quad (7)$$

Here, $\lambda(r)$ are the values of the envelope parameter and λ_{min} and λ_{max} are bounds that are determined by the constraints on the pulse duration T_s. The FM rate values for each $\lambda(r)$ and for each considered waveform $\mathcal{W}^1, \ldots, \mathcal{W}^{\mathcal{K}}$, are given by $b(m)$ where b_{max} is the maximum possible FM rate which is obtained from Table 1 by using the same fixed bandwidth B. Thus, each sensor has $RM\mathcal{K}$ possible configurations obtained by varying the waveforms and their parameters and $L = (RM\mathcal{K})^2$. Note that if one of the $\mathcal{K}$ waveforms is a Gaussian pulse, there is no FM rate associated with it and $L = (RM(\mathcal{K}-1)+R)^2$. For LFM chirps only, we also considered stochastic optimization for this 2-D problem in [7]. Though the performance is comparable, the stochastic approximation approach was more computationally intensive than the new proposed algorithm.

5. SIMULATION RESULTS

The simulation setup consists of a single underwater target that is free to move in a 2-D plane. The carrier frequency is ω_c = 25 kHz and the velocity of sound in water is 1500 m/s.

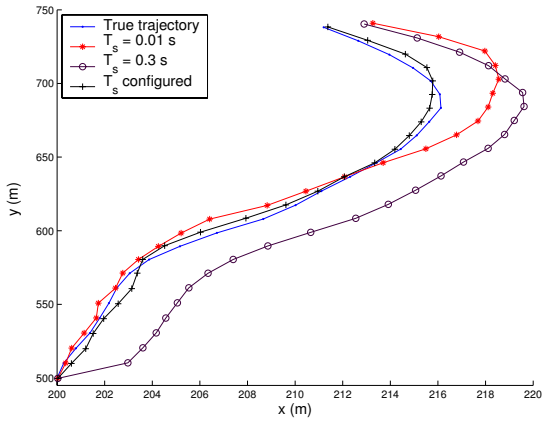

Fig. 1. Position estimate of the target in Example 1. Sensors A and B are located at (200,975) and (0,220) m.

The effective pulse length, T_s, is chosen to be the time interval over which the signal amplitude is greater than 0.1% of its maximum value. This further determines the value of $\lambda = T_s/\alpha$, where $\alpha = 7.4338$. For all waveforms, the pulse length is constrained to lie in the range [0.01,0.3] s while the bandwidth is limited to $B = 5$ kHz. We assume perfect target detection and zero probability of false alarm.

Example 1. We first test the waveform parameter selection algorithm by choosing λ for a single Gaussian waveform. The SNR at a distance r from a sensor is $\eta = (1000/r)^4$. Fig. 1 shows the trajectory of the target and a typical simulation of the estimates of its position obtained when the sensors use waveforms with fixed durations of 0.01 s and 0.3 s, and when the duration is dynamically selected. The selected pulse length and the tracking mean square error (MSE) averaged over 100 simulations are shown in Fig. 2.

Example 2. In this example, the two sensors independently choose between the $\mathcal{K} = 3$ waveforms in Table 1. Our simulations showed that the lowest cost for a particular waveform is obtained when its parameters are set to their limiting values as defined by the system constraints. In (6), $R = 2$ so that $\lambda(r) = 0.0013$, 0.404, and in (7) we set $M = 3$. For the HFM pulse, b_{max} is set to the maximum allowable FM rate, which, for the purpose of the simulation, was set to 500000. We further require that $T = B/b_{max}$. The SNR at distance r is $\eta = (175/r)^4$. Fig. 3 shows a comparison of the total MSE, averaged over 100 simulations, when the target in Fig. 1 is tracked using the three pulses with our proposed algorithm. We find that the waveform selected is the HFM pulse with the maximum possible value of λ.

6. DISCUSSION

When the waveform is only parameterized by its pulse length, as with the Gaussian pulse in Example 1, the measurement errors for position increase while those for velocity decrease with increasing pulse length. The errors are also uncorrelated. This opposing behavior leads to a trade-off between

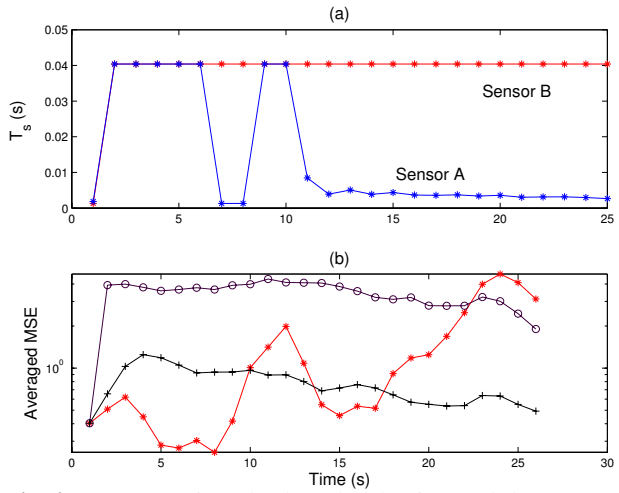

Fig. 2. (a) Dynamic pulse length selection and (b) averaged tracking error for the waveform selected in Example 1. In (b), $T_s = 0.01$ s $(*)$, $T_s = 0.3$ s $(\circ)$ and configured T_s $(+)$.

the accuracy of range and range-rate estimation which the tracker exploits by dynamically selecting the waveform pulse length that results in the lowest total tracking error. For the GFM waveforms in Example 2, the estimation errors are correlated. When the measurement noise is Gaussian, the conditional variance for range-rate errors given the range may be shown to be $\sigma^2_{\dot{r}|r} = 2c^2/(4\eta\omega_c^2\lambda^2)$ for all pulses. The conditional variance on range errors given the range-rate, $\sigma^2_{r|\dot{r}}$, depends upon $g(\xi)$ in (4). It is approximately obtained from $N(\boldsymbol{\theta}_k)$ as

$$\text{LFM:}\quad \frac{c^2}{4\eta B^2}\frac{\alpha^2}{2}, \quad \text{EFM:}\quad \frac{c^2}{4\eta B^2}\frac{e^{\lambda(\alpha-\lambda)}}{(1+\text{erf}(\lambda))},$$
$$\text{HFM:}\quad \frac{c^2}{4\eta B^2}\frac{1}{T^2\int_{-\infty}^{\infty}\frac{1}{\lambda\sqrt{\pi}}e^{-\frac{t^2}{\lambda^2}}\frac{1}{(T+|t|)^2}dt}. \qquad (8)$$

Intuitively, the configuration algorithm must choose the waveform for which $\sigma^2_{r|\dot{r}}$ is the smallest. From Table 1, the FM rate for the HFM pulse is not constrained by the value of λ (and thus T_s) in contrast to the LFM and EFM pulses. Thus, it can always be chosen as the maximum allowed value. For a given B, T can be chosen large and $\sigma^2_{r|\dot{r}}$ in (8) is the lowest for the HFM waveform. It thus provides the best tracking performance as demonstrated in Fig. 3.

7. CONCLUSION

Most realistic tracking applications are characterized by nonlinearities. The difficulty of predicting costs in closed form in such scenarios complicates the optimal waveform selection problem. In this work, we have shown that it is possible to select the next transmitted waveform on the basis of an expected predicted cost in a computationally feasible manner using the unscented transform and a grid search.

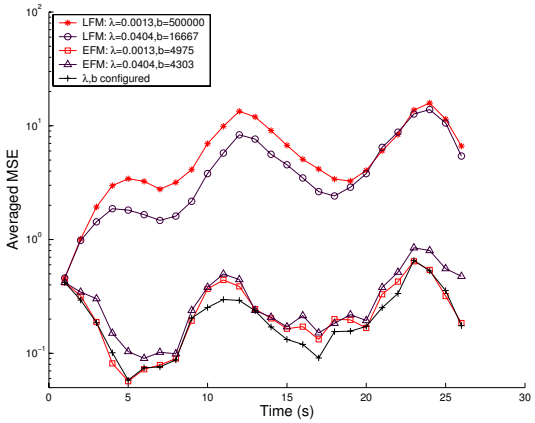

Fig. 3. Averaged MSE using fixed and configured waveforms and waveform parameters.

We have applied the selection algorithm to the tracking of an underwater target by two fixed sensors using a class of GFM waveforms. Two simulation examples demonstrate the capabilities of the proposed algorithm.

8. REFERENCES

[1] B. F. La Scala, W. Moran, and R. J. Evans, "Optimal adaptive waveform selection for target detection," in *Int. Conf. on Radar*, 2003, pp. 492–496.

[2] D. J. Kershaw and R. J. Evans, "Optimal waveform selection for tracking systems," *IEEE Trans. on Information Theory*, vol. 40, pp. 1536–1550, Sept 1994.

[3] D. J. Kershaw and R. J. Evans, "Waveform selective probabilistic data association," *IEEE Trans. on Aerospace and Electronic Systems*, vol. 33, pp. 1180–1188, Oct 1997.

[4] S-M. Hong, R. J. Evans, and H-S. Shin, "Optimization of waveform and detection threshold for target tracking in clutter," in *SICE Annual Conference*, July 2001, pp. 42–47.

[5] A. Papandreou-Suppappola and S. B. Suppappola, "Sonar echo ranging using signals with non-linear time-frequency characteristics," *IEEE Sig. Proc. Letters*, vol. 11, March 2004.

[6] S. Julier and J. Uhlmann, "A new extension of the Kalman filter to nonlinear systems," *Int. Symp. Aerospace/Defense Sensing, Simul. and Controls*, 1997.

[7] S. P. Sira, D. Morrell, and A. Papandreou-Suppappola, "Waveform design and scheduling for agile sensors for target tracking," *Asilomar Conf. on Signals, Systems and Computers*, November 2004.

[8] R. van der Merwe, N. de Freitas, A. Doucet, and E. Wan, "The Unscented Particle Filter," Tech. Rep. CUED/F-INFENG/TR380, Cambridge University, Aug. 2000, `http://citeseer.ist.psu.edu/article/vandermerwe00unscented.html`.

[9] H. L. Van Trees, Ed., *Detection Estimation and Modulation Theory, Part III*, Wiley, New York, 1971.